ANALYSIS AND OPTIMIZATION OF UNDERACTUATED FINGER FOR CMSYSLAB ROBOTIC HAND

Miloš D. Lukić, student PhD[1], Mihailo P. Lazarević[1], Petar B. Petrović[1]

[1]Faculty of Mechanical Engineering,
The University of Belgrade, Kraljice Marije 16, 11120 Belgrade 35
e-mail: mlukic@mas.bg.ac.rs, pbpetrovic@mas.bg.ac.rs, mlazarevic@mas.bg.ac.rs

Abstract:

In this paper is presented mathematical analysis of 3-DOF underactuated robotic finger with linkage driven mechanism. The optimization procedure is described for obtaining optimal parameters of four bar mechanism. As results, the adaptability of the finger is improved and the grasping forces maximized within the working area limits.

Key words: robotic hand, underactuation, linkage, optimization,

1. The concept of underactuation

Underactuation of mechanical systems represent case when system has fewer actuators than degrees of freedom. In case of robotic grasping, underactuation allows the robotic hand to adjust itself to irregularly shaped object, without complex control strategies and sensors [1]. This approach can also greatly reduce the number of actuator elements, simplifying the control process [2-4].

1.1 General case of underactuated finger with n-DOF, and one degree of actuation

In Fig.1 is ilustrated underactuated finger with *n* phalanges. The input torque from actuator is applied to the first joint of the finger, and it is transmitted to the phalanges through four-bar linkages. Adding the springs to the joints results with fully adaptive finger with compliant joints. Passive elements are used to kinematically constrain the finger, and to ensure that finger will adapt to the shape of object being grasped.

In order to determine the distributions of the contact forces that depend on the contact point location and the joint torques inserted by springs, it is necessary to perform a static modeling of the finger. Assumptions are made that the friction must be ignored and the grasping object has to be fixed.

As result of the static modeling, as shown in [5], it is obtained:

$$F = J_T^{-T} J_a^{-T} T \,, \tag{1}$$

where J_a represents actuation Jacobian matrix, J_T is Jacobian matrix of projected velocities, and T represents the input torque vector from the actuator and springs. This represents equation that provides a practical relationship between the actuator torques and contact forces. Equation is only valid in case when positions of the contact points $k_1 k_2 k_3 \ldots k_n \neq 0$, which is the condition of singularity for matrix J_T.

1.2 Stability analysis of the grasp in case of 3-DOF underactuated finger

In Fig. 2 are described geometric and force parameters of underactuated 3-DOF finger, while on Fig. 3 is shown real structure design of CMSysLab hand finger. Parameters of the finger are illustrated on Table 1. The behavior of the finger is mostly determined by its geometry.

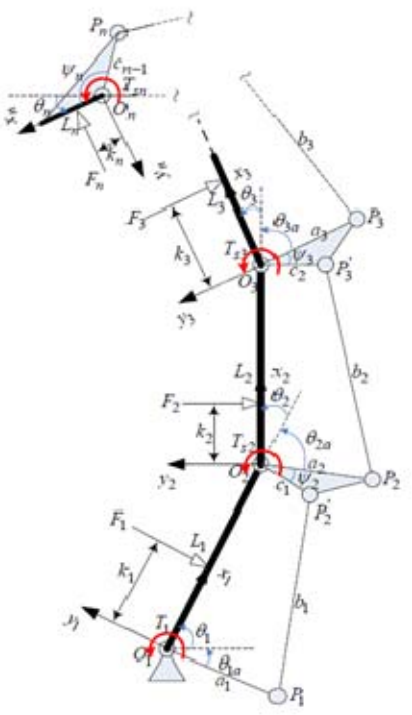

Fig. 1. Parameters of underactuated n-DOF finger

Depending on the geometric parameters of the mechanism, it is possible to obtain the final stability of the grasp. The grasping forces obtained from actuator are primarily dictated by two factors. One is the configuration of the finger, described by angles between phalanges θ_2 and θ_3. The other factor is the contact locations on the phalanges, described by force arms k_1, k_2 and k_3.

In earlier papers, it is shown that that θ_3 impacts the force magnitudes more distinctly that θ_2 does. Increasing of θ_3 leads to decreasing of F_1 and F_3 but increment of F_2.

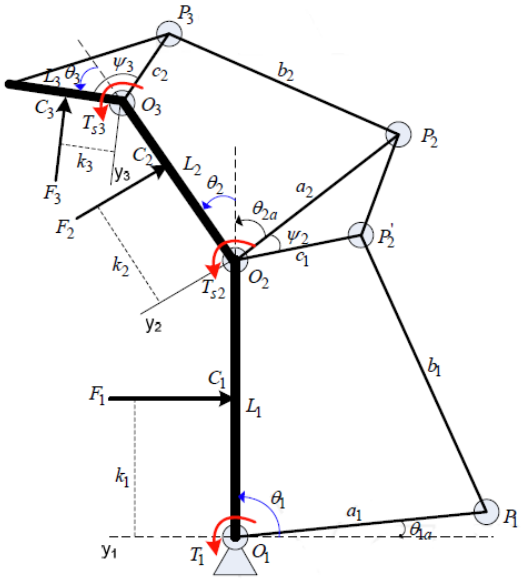

Fig. 2. Geometric and force parameters of underactuated 3-DOF finger

The effect of θ_2 is complex, and it depends on geometric parameters of the mechanism. The example of the stability grasp is shown on Fig. 4, by finding the planes where the forces equal to zero. A stable grasp refers to a positive force on the phalanx. If the force is negative, the corresponding phalanx might slide on the object or lose contact with the object.

In most cases of a multi-fingered grasp, only force on the distal phalanx i.e. F_3 needs to be positive. Due to kinematical design, F_3 is always positive. Therefore, the three-phalanx CMSysLab finger has good grasp stability. As earlier mentioned, it is concluded that the choice of the design parameters is very important in order to provide stable grasps and a proper distribution of the forces among the phalanges. It is shown that the behavior of the fingers is mainly dictated by the ratios:

$$R_i = \frac{a_i}{c_i},\ i = 1,2\,. \tag{2}$$

Criteria used for determining performance of the fingers can also be evaluated with global performance index. The graph of the global performance index is a function of R_1 and R_2 parameters. Among the best values, the most effective finger with stable grasps could be chosen.

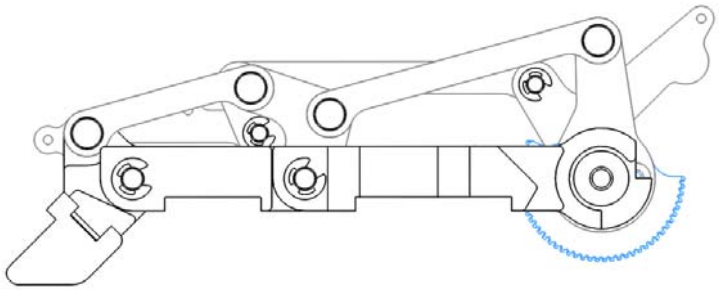

Fig. 3. The structure design of the CMSysLab hand finger

In structure of the finger, mechanical limit is used, which allows a pre-loading of the spring to prevent any undesirable motion of the medial and distal phalanges, due to its own weight and/or inertial effects, as well to prevent hyperflexion of the finger [6].

a_1 [mm]	30	a_2 [mm]	23
b_1 [mm]	60.5	b_2 [mm]	37
c_1 [mm]	15	c_2 [mm]	14
L_1 [mm]	64.5	ψ_2 [degree]	52
L_2 [mm]	37.5	ψ_3 [degree]	90
L_3 [mm]	34.5		

Table 1. Parameters of the CMSysLab hand finger

The set of parameters presented in Table 1 is taking into account the mechanical joint limits, which are key elements in the design of underactuated fingers, when considering stability issues, because they limit the shape adaptation to reasonable configurations (thus reducing the possibility of ejection).

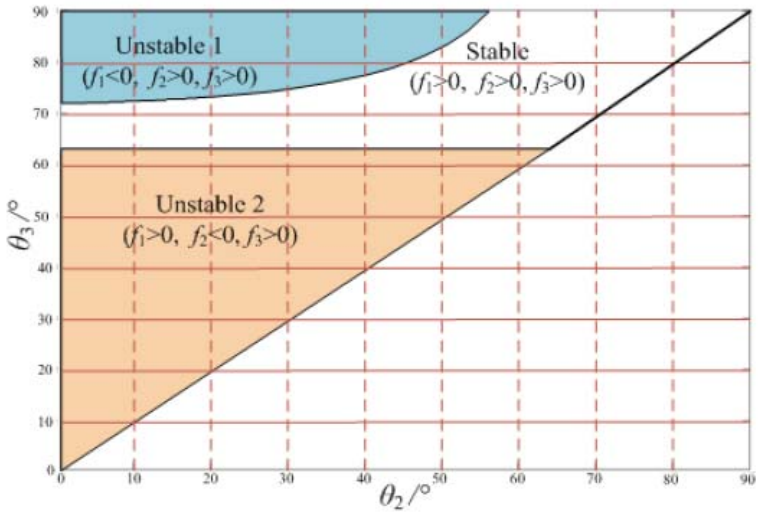

Fig. 4. Grasping stability of the three phalanx underactuated finger

2. The general contact force analysis of underactuated finger

2.1 Case of 3-DOF finger with one degree of actuation

In case of the underactuated finger with 3-DOF, Eq.(1) holds if and only if $k_1 k_2 k_3 \neq 0$, which represents the condition of singularity for the matrix J_T, as shown in Fig.5a. There are however and other cases, when finger can contact the object when one or two phalanges of the finger not touching the object, which is shown in Fig. 5b, 5c and 5d.

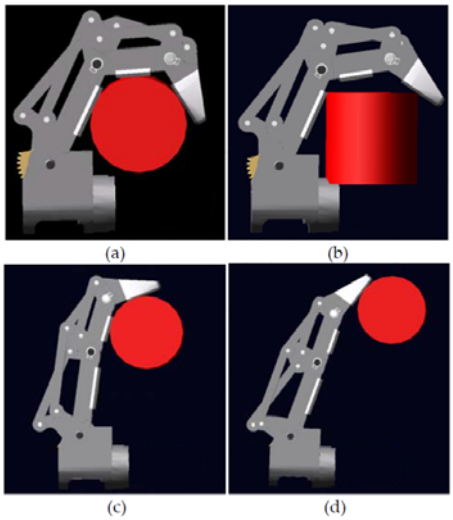

Fig. 5. Four cases of finger grasping

In order to calculate the contact forces F_1, F_2 and F_3 on the grasping object, it is necessary to separate four cases of possible behaviors between the finger and the object during grasping process, as shown in Fig.4.

Case 1: All three phalanges of the finger are in contact with the object, so $k_1 k_2 k_3 \neq 0$, as shown in Fig. 5a. The relationship between the actuator torques and contact forces can be derived from equation for case of n-DOF finger with one degree of actuation:

$$\begin{bmatrix} k_1 & 0 & 0 & \cdots & 0 \\ \alpha_{12} & k_2 & 0 & \cdots & 0 \\ \alpha_{13} & \alpha_{23} & k_3 & \cdots & 0 \\ \cdots & \cdots & \cdots & \cdots & \cdots \\ \alpha_{1n} & \alpha_{2n} & \alpha_{3n} & \cdots & k_n \end{bmatrix}^T \begin{bmatrix} F_1 \\ F_2 \\ F_3 \\ \cdots \\ F_n \end{bmatrix} = \begin{bmatrix} \tau_1 \\ \tau_2 \\ \tau_3 \\ \cdots \\ \tau_n \end{bmatrix}, \tag{3}$$

which shows that the torque τ_i at the i^{th} joint of the finger is calculated with respect to the contact forces vector F and parameters α_{ij}, as shown in following equation:

$$\sum_{j=i}^{n} \alpha_{ij} F_j = \tau_i, \quad \alpha_{ii} = k_i . \tag{4}$$

From (3), the relationship between the actuator torques and contact forces can be derived for case of 3-DOF finger with one degree of actuation:

$$\begin{bmatrix} k_1 & k_2 + L_1 C_2 & k_3 + L_1 C_{23} + L_2 C_3 \\ 0 & k_2 & k_3 + L_2 C_3 \\ 0 & 0 & k_3 \end{bmatrix} \begin{bmatrix} F_1 \\ F_2 \\ F_3 \end{bmatrix} = \begin{bmatrix} T_1 \\ T_{s2} - X_1 T_1 \\ T_{s3} - X_2 T_{s2} + X_1 X_2 T_1 \end{bmatrix}. \tag{5}$$

From previous equation, the three contact forces F_1, F_2 and F_3 can be easily computed.

Case 2: The proximal and distal phalanges are in contact with the object, which means that parameter k_2 does not exist, while force F_2 is zero, as illustrated in Fig. 5b.

In (5), the second column and second row in the matrix J_T relating to the medial phalanx are removed, as well as the force F_2 and the torque $\tau_2 = T_{s2} - X_1 T_1$ in the vectors F and τ. After removal of aforementioned elements, (5) obtains the following form:

$$\begin{bmatrix} k_1 & k_3 + L_1 C_{23} + L_2 C_3 \\ 0 & k_3 \end{bmatrix} \begin{bmatrix} F_1 \\ F_3 \end{bmatrix} = \begin{bmatrix} T_1 \\ T_{s3} - X_2 T_{s2} + X_1 X_2 T_1 \end{bmatrix}. \tag{6}$$

Case 3: The medial and distal phalanges are in contact with the object, which means that parameter k_1 does not exist, while force F_1 is zero, as illustrated in Fig. 5c.

In Eq.(3), the first column and first row in the matrix J_T relating to the proximal phalanx are removed. Also, the elements F_1 and τ_1 in the force vector F and torque vector τ are removed. Then, (3) becomes:

$$\begin{bmatrix} k_2 & k_3 + L_2 C_3 \\ 0 & k_3 \end{bmatrix} \begin{bmatrix} F_2 \\ F_3 \end{bmatrix} = \begin{bmatrix} T_{s2} - X_1 T_1 \\ T_{s3} - X_2 T_{s2} + X_1 X_2 T_1 \end{bmatrix}. \tag{7}$$

Case 4: Only the distal phalanx is in contact with the object, which means that parameters k_1 and k_2 do not exist, while elements F_1 and F_2 of force vector F are zero, as illustrated in Fig. 5d.

In Eq. (3), the first and second column and row in the matrix J_T relating to the proximal and medial phalanges are removed, as well as the elements F_1 and F_2 of the force vector F, and element τ_2 of the torque vector τ. Then, Eq.(3) becomes:

$$k_3 F_3 = T_{s3} - X_2 T_{s2} + X_1 X_2 T_1 \tag{8}$$

3. Optimization of segments of the linkage driven mechanism

Simplified sketch of underactuated 3-DOF finger with linkage driven mechanism is shown on Fig. 6. The optimal dimensional synthesis of the linkage driven mechanism shown in Fig. 6, which is used as transmission system from the electric motor to the three phalanxes of the proposed underactuated finger, is formulated by using the Freudenstein's equations [7] and the transmission defect, as index of merit of the force transmission.

The three linkages connected in series are synthesized by starting from the four bar linkage which moves the third phalanx.

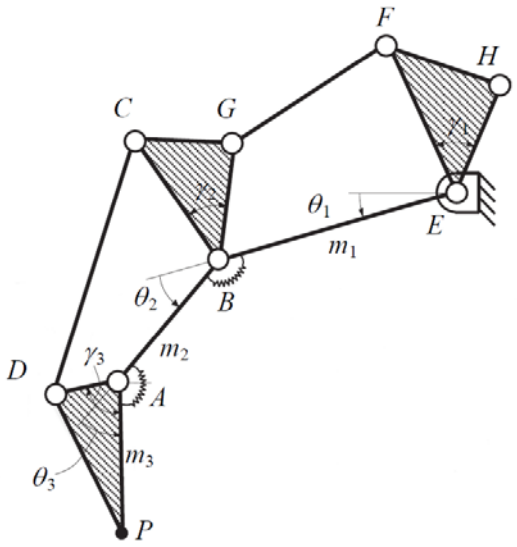

Fig. 6. Kinematic sketch of the underactuated finger mechanism

3.1 *Synthesis of the four bar linkage B, E, F ,G*

By considering the four-bar linkage *BEFG* in Fig. 6 and Fig. 7, the Freudenstein's equations can be expressed in the following form [8]:

$$R_1 \cos\psi_i - R_2 \cos\varphi_i + R_3 = \cos(\psi_i - \varphi_i), \quad i = 1, 2, 3, \tag{9}$$

with coefficients of Freudenstein's equation:

$$R_1 = \frac{l_1}{d}, \quad R_2 = \frac{l_1}{f}, \quad R_3 = \left(d^2 - e^2 + f^2 + l_1^2\right) / 2df, \tag{10}$$

where l_1 represents the length of the first phalanx, d, e and f are the lengths of the links *BG*, *GF* and *EF* respectively, and ψ_i and φ_i for $i = 1, 2, 3$ are the input and output angles of the four bar linkage *BEFG*.

Likewise to the four-bar linkage *BEFG*, Eq.(9) can be solved when three positions 1), 2) and 3) of both links *EF* and *BG* are given through the pairs of angles (ψ_i, φ_i) for $i = 1,2,3$.

In particular, according to a suitable mechanical design of the underactuated 3-DOF finger, following design parameters are assumed: $\gamma = -80^\circ$, $\beta_2 = -48^\circ$ and $\delta = 7.5^\circ$.

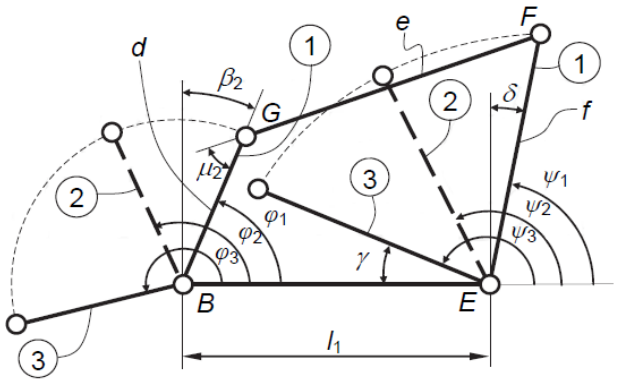

Fig. 7. Four bar linkage BEFG

Consequently, the pairs of angles $(\psi_1, \varphi_1) = (94^\circ, 90^\circ)$ and $(\psi_3, \varphi_3) = (260^\circ, 300^\circ)$ are obtained for the starting 1) and final 3) positions of four bar linkage mechanism. Since only two of the three pairs of angles required by the Freudenstein's equations are assigned as design specification of the function-generating four-bar linkage *BEFG*, an optimization procedure in terms of force transmission has been developed by varying values of (ψ_2, φ_2) during process of optimization. The transmission quality of the four-bar linkage is shown in the following equation:

$$z = \int_{\psi_1}^{\psi_3} \cos^2 \mu_2 \, d\psi \,. \tag{11}$$

The transmission defect is described by:

$$z' = \frac{1}{\psi_3 - \psi_1} \int_{\psi_1}^{\psi_3} \cos^2 \mu_2 \, d\psi \,, \tag{12}$$

where μ_2 represents the transmission angle, which is expressed by following equation:

$$\mu_2 = \cos^{-1}\left(\frac{l_1^2 + f^2 - d^2 - e^2 - 2 l_1 \, \mathrm{f} \cos(\pi - \psi)}{2de} \right). \tag{13}$$

The optimal values of the pair of angles (ψ_2, φ_2) are obtained through the optimization of the transmission defect z'.

Optimization process can be described in the following steps:

- Defining the base phalanx length l and pairs of minimum and maximum values of the input and output angles (ψ_1, φ_1) and (ψ_3, φ_3) of four bar linkage;

- Substitution of angle pairs (ψ_1, φ_1), (ψ_3, φ_3), and values of ψ_2 and φ_2, in the Freudenstein's equations;
- Symbolic solving the system of three equations, resulting in a equations for lengths d, e and f, which are in function of angles ψ_2 and φ_2;
- Varying the angles ψ_2 and φ_2, from minimum (ψ_1, φ_1) to maximum (ψ_3, φ_3) values, with previously defined incremental steps. With every transition of double *FOR* loop, obtained values of segment lengths are written in matrices D, E and F. At the same time, the value of transmission defect z' is calculated, whose values are entered into a matrix Z;
- Finding the minimum element of the matrix Z, and reading the number of iterations for angles ψ_2 and φ_2 for which the minimum value is obtained;
- For number of iterations for which the minimum value of transmission defect z' is obtained, optimal values of four bar linkage lengths are read out from matrices D, E and F.

Due to a technical feasibility, the following constraints for segment lengths have been adopted:

$$25 < d < 50;\ 40 < e < 70;\ 10 < f < 60. \tag{14}$$

After the optimization, the optimal values for lengths of the four bar linkage segments are obtained: $d = 25.0227\,mm$, $e = 54.285\,mm$ and $f = 37.1171\,mm$, while the value of transmission defect is $z' = 0.4658$.

On Fig.8 is shown the 3D plot of the transmission defect matrix Z, while plot with zones of local minimum of z' is shown on Fig.9.

On Fig.9, zone with values of local minimum are marked with deep blue color.

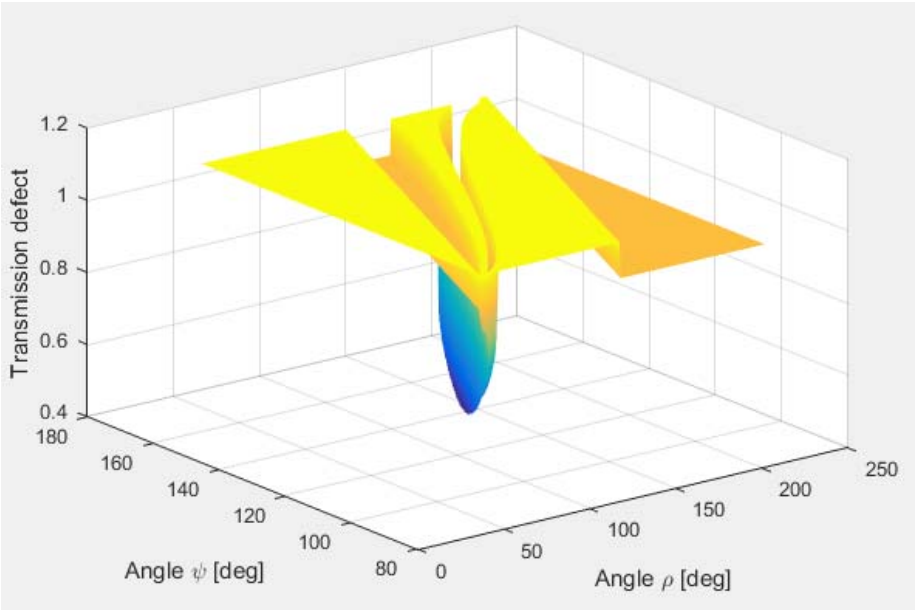

Fig. 8. Changes of values of transmission defect z' with variations of angles ψ_2 and φ_2.

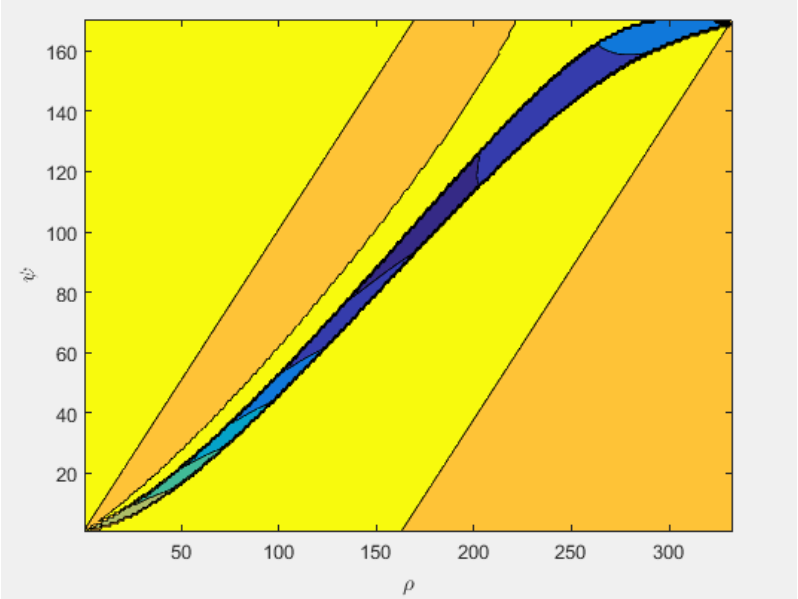

Fig. 9. Zones of local minimum of transmission defect z'

On Fig. 10 is shown four bar linkage BEFG, with optimized segment lengths.

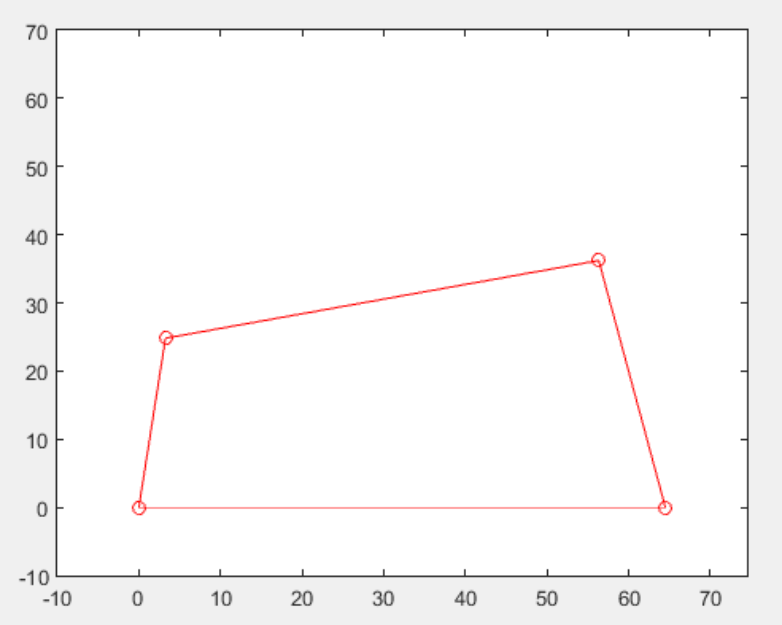

Fig. 10. Four bar linkage with optimized segments

3. Conclusions

This paper presents a mathematical analysis to determine the distribution of contact forces for the underactuated finger in general grasping cases of an underactuated robotic hand.

Also, presented optimization method gives lower transmission defect values than the ordinary methods for the same design specifications. Consequently the adaptability of the finger is improved and the grasping forces maximized within the working area limits.

Usually, the design was mainly driven by the designer's inspiration which can result in good design and often poor results. Presented optimization method can be used to design fingers using linkages as transmission mechanism, and it can ensure the optimality of design with respect to grasping characteristics.

Aknowledgment

This research was partially supported by the research grant of the Serbian Ministry of Education, Science and Technological Development under the number TI 35006.

References

1. C.M. Gosselin and T. Lalibertè, *Underactuated Mechanical Finger with Return Actuation*, U.S. Patent 5 762 390, 1998.
2. L. Birglen, T. Lalibertè and C. Gosselin, *Underactuated robotic hands*, pp. 345-360 (B.Siciliano and O. Khatib, F. Groen, Eds, Springer Tracts in Advanced Robotics. Berlin: Spinger), 2008.
3. T. Lalibertè, L. Birglen and C.M. Gosselin, *Underactuation in robotic grasping hands*, Machine Intelligence and Robotic Control, Vol. 4, No. 3, 1-11, 2002.
4. W. Townsend, The BarrettHand grasper - programmably flexible part handling and assembly, vol. 27 (3), pp. 181-188 (Ind. Rob.), 2000.
5. Birglen, L. and Gosselin, C.M., *Kinetostatic analysis of underactuated fingers*. IEEE Transactions on Robotics and Automation: 20, 211-221, 2004.
6. Rea, P., *On the design of underactuated finger Mechanisms fo robotic Hands*. In H. M. Alfaro (Ed.), Advances in Mechatronics. doi:10.5772/875, 2011.
7. Freudenstein, F., *Design of Four-link Mechanisms,* Ph. D. Thesis, Columbia University, USA, 1954.
8. Hartenberg, R. S., & Denavit, J., *Kinematic synthesis of Linkages*. (S. M.Drake, Robert, JR, J.Kline, Ed.), 1964.